On the $\sigma(\chi_{c1})/\sigma(\chi_{c2})$ ratio in the k_t-factorization approach

S. P. Baranov*
P.N. Lebedev Institute of Physics, Lenin Avenue 53, Moscow 119991, Russia
(Dated: December 2, 2010)

We address the puzzle of $\sigma(\chi_{c1})/\sigma(\chi_{c2})$ ratio at the collider and fixed-target experiments. We consider several factors that can affect the predicted ratio of the production rates. In particular, we discuss the effect of χ_{cJ} polarization, the effect of including next-to-leading order contributions, and the effect of probably different χ_{c1} and χ_{c2} wave functions.

PACS numbers: 12.38.Bx, 13.85.Ni, 14.40.Pq

I. INTRODUCTION

Since it was first observed, charmonium production in hadronic collisions has been a subject of considerable theoretical interest. Charmonim production rates and their dependence on the different kinematic variables provide important tests for comparing theoretical models. The ratios of the production rates are of no less concern. While the predictions on the absolute production cross sections may vary significantly with the input gluon densities, the renormalization and factorization scales, the quark mass value, etc., the ratios of the production rates are more stable (as the corresponding factors cancel out in the ratio) and may be regarded as even better indicators of the production mechanism on its own.

This note is largely inspired by the experimental measurement of the ratio of the χ_{cJ} production cross sections reported by the CDF Collaboration at the Fermilab Tevatron [1]: $[\sigma(\chi_{c2})B_{\psi\gamma}(\chi_{c2})]/[\sigma(\chi_{c1})B_{\psi\gamma}(\chi_{c1})] = 0.395 \pm 0.016(\text{stat}) \pm 0.015(\text{syst})$. This result provides the most precise measurement of the χ_{cJ} production ratio obtained in any hadronic interaction. Among the fixed-target experiments, the absolutely largest statistics has been collected by the HERA-B Collaboration at DESY HERA [2]. The reported result is $\sigma(\chi_{c1})/\sigma(\chi_{c2}) = 0.57 \pm 0.23$.

Apparently, these numbers are at odds with naive theoretical expectations appealing to Landau-Yang theorem and implying strong suppression of χ_{c1} states. It would be inadequate, however, to make comparisons paying no attention to experimental conditions. In fact, experimental acceptance selects some specific kinematical region where the visible ratio of the production rates may be different from the one averaged over the unrestricted phase space.

The goal of this note is to carefully examine the situation and see to what extent can the experimental data be accommodated by theoretical calculations. We also wish to guess what can be done in the theory to reach a better level of agreement with the data.

*Electronic address: baranov@sci.lebedev.ru

II. THEORETICAL FRAMEWORK

Our calculations are based on the standard QCD perturbation theory and nonrelativistic bound state formalism of Refs. [3]. In the k_t-factorization approach, we consider the partonic subprocess

$$g^* + g^* \to \chi_{cJ}, \quad J = 0, 1, 2 \tag{1}$$

that represents the leading-order (LO) QCD contribution. In the case of collinear factorization, the leading order is represented by the 2→2 subproces

$$g + g \to \chi_{cJ} + g, \quad J = 0, 1, 2 \tag{2}$$

as the 2→1 subprocess (1) would lead to unphysical δ-like p_T distributions. The corresponding Feynman diagrams are presented in Fig. 1.

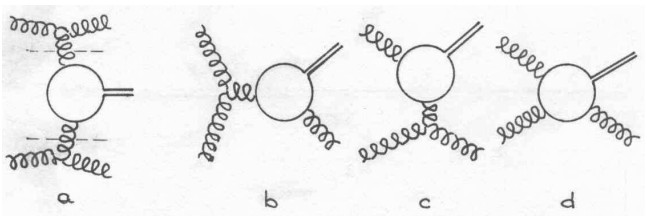

FIG. 1: Feynman diagrams representing the hadronic production of χ_{cJ} mesons in the k_t-factorization approach **(a)** and leading-order collinear calculations **(b)-(d)**. The central part of diagram **(a)** represents the partonic subprocess (1) where the initial gluons have nonzero transverse momentum generated in the course of parton evolution (the upper and the lower parts of the diagram).

The amplitudes of the partonic subprocesses (1) and (2) contain spin projection operators that guarantee the proper quantum numbers of the $c\bar{c}$ bound states. We strictly follow the color-singlet production scheme. The details of calculations are explained in Refs. [4, 5]. For the sake of definiteness, we only present here the parameter setting. Throughout this note, we use the leading-order GRV (Glück-Reya-Vogt) set [6] for collinear gluon density in the proton. For the unintegrated gluon densities we use the parametrization proposed in Ref. [7] (hereafter called JB) with collinear GRV set taken as input and, also, the A0 parametrization from Ref. [8] representing a numerical fit to the available HERA data

based on CCFM equation [9]. The renormalization and factorization scales are set to $\mu_R^2 = \mu_F^2 = m_\chi^2 + p_T^2$, the charmed quark mass $m_c = m_\chi/2 = 1.7$ GeV, and the value of the χ_{cJ} wave function $|\mathcal{R}'_\chi(0)|^2 = 0.075$ GeV^3 is taken from the potential model of Ref. [10]. The integration over the final state phase space is restricted to the pseudorapidity and x_F intervals specified by the CDF and HERA-B Collaborations.

It is worth mentioning that comparisons with the data need some delicacy as the produced mesons are polarized. Polarization affects the angular distributions of the decay products and, consequently, affects the efficiency of their detection. Our further predictions depend on the properties of the decays $\chi_{cJ} \to J/\psi + \gamma$. Uncertainties coming from the related theoretical models have been discussed in Ref. [11]. Under the assumption that these decays are dominated by the electric dipole transitions [12], the photon angular distributions read

$$\frac{d\Gamma(\chi_{c1}\to\psi\gamma)}{d\cos\theta} \propto \left[\left(1+\tfrac{1}{2}\rho\right) + \left(1-\tfrac{3}{2}\rho\right)\cos^2\theta\right], \qquad (3)$$

$$\frac{d\Gamma(\chi_{c2}\to\psi\gamma)}{d\cos\theta} \propto \left[\left(\tfrac{5}{6}-\tfrac{1}{12}\xi-\tfrac{1}{3}\tau\right) - \left(\tfrac{1}{2}-\tfrac{1}{4}\xi-\tau\right)\cos^2\theta\right]$$

where $\rho = d\sigma(\chi_{c1}^{|h|=1})/d\sigma(\chi_{c1})$, $\xi = d\sigma(\chi_{c2}^{|h|=1})/d\sigma(\chi_{c2})$, $\tau = d\sigma(\chi_{c2}^{|h|=2})/d\sigma(\chi_{c2})$, and θ is the angle between the photon momentum (measured in the χ_{cJ} rest frame) and a chosen reference axis. For the unpolarized χ_{c1} and χ_{c2} mesons one would have $\rho = 2/3$, $\xi = \tau = 2/5$, and the photon angular distribution would be uniform.

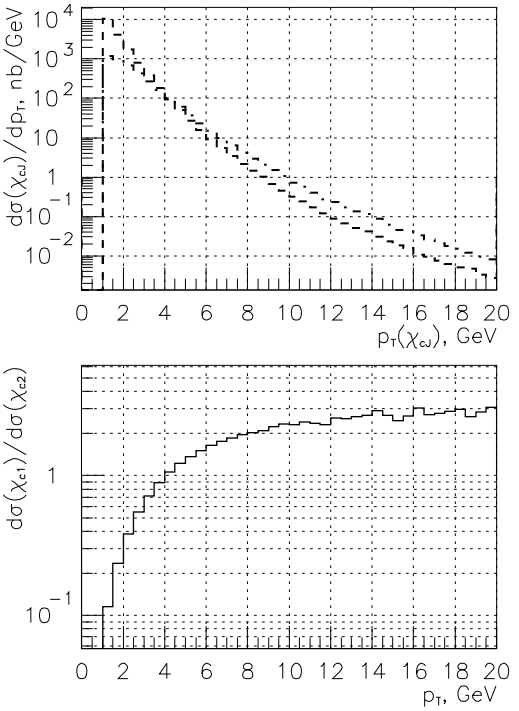

FIG. 2: Leading-order colinear predictions for the Tevatron conditions: $\sqrt{s} = 1.96$ TeV, $|\eta(\chi_{cJ})| < 1$. Upper panel, transverse momentum distributions of the χ_{c1} (dash-dotted line) and χ_{c2} (dashed line) mesons. Lower panel, the ratio of the χ_{c1} and χ_{c2} production cross sections.

III. COMPARISON TO THE TEVATRON DATA

Prior to discussing the k_t-factorization approach, we find it useful to recall some basic results obtained within the collinear factorization scheme: the latter is regarded by the scintific community as a kind of "standard" theory. Fig. 2 displays the LO QCD predictions for the χ_{cJ} differential cross sections and their ratio.

The requirement that the transverse momentum of the photon emerging from the decay $\chi_{cJ} \to J/\psi+\gamma$ be greater than 1 GeV [1] implies that the transverse momentum of the decaying meson be greater than approximately 5 GeV, and, respectively, the p_T of the produced J/ψ meson greater than 4 GeV. Here the suppression of χ_{c1} states seen at low p_T goes away, and the ratio $d\sigma(\chi_{c1})/d\sigma(\chi_{c2})$ then tends to a constant value.

Fig. 3 shows the spin alignement parameters ρ, ξ, and τ in the helicity frame. In the Collins-Soper frame, the absolutely dominating polarizations are $h = \pm 1$ for χ_{c1} mesons and $h = \pm 2$ for χ_{c2} mesons. (The spin density matrix is the same in all cases, and the difference in the polarization parameters is only due to differently chosen reference axes.)

Having generated the χ_{cJ} decays in accordance with their polarization properties and imposing the restriction $p_T(\gamma) > 1$ GeV we arrive at the plots exhibited in Fig. 4, nicely compatible with the experimental results. At the same time, the predictions on the shape of the differential cross section show a wrong p_T dependence (Fig. 5 with the data from Ref. [13]). This fact necessitates including higher order contributions.

Performing the full next-to-leading order (NLO) calculations requires quite a significant work. It has been done recently in Ref. [14]. The authors report on the change in the p_T behavior in the color-singlet channels: it scales as $1/p_T^4$ at the NLO in contrast with $1/p_T^6$ at LO. The authors also find that at relatively large p_T the NLO color-singlet contributions become negative, and so, to keep the production cross sections positive they call for color-octet contributions. Thus, the solution of the problem is laid upon nonperturbative and essentially uncalculable color-octet mechanism.

Over the years, nobody was able to estimate the relevant color-octet matrix elements within the context of the theory, even approximately. In all its applications, the color-octet model has never been anything more but a collection of unpredictable fitting parameters. And so far, it fails to provide a self-consistent fit of the Tevatron and HERA data. "Solutions" appealing to the color-octet model tell very little about physics.

With the k_t-factorization approach, we hope to preserve the perturbative nature of the theory. Even with the LO matrix elements, the correct p_T behavior of the

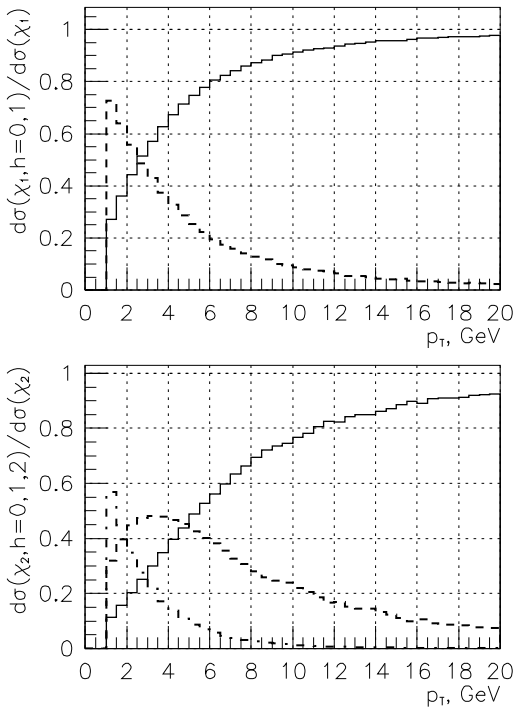

FIG. 3: Leading-order colinear predictions on the χ_{cJ} spin alignement parameters at the Tevatron as seen in the helicity frame. Upper panel, χ_{c1} mesons; lower panel, χ_{c2} mesons. Solid lines, $h = 0$ states; dashed lines, $|h| = 1$ states; dash-dotted line, $|h| = 2$ states.

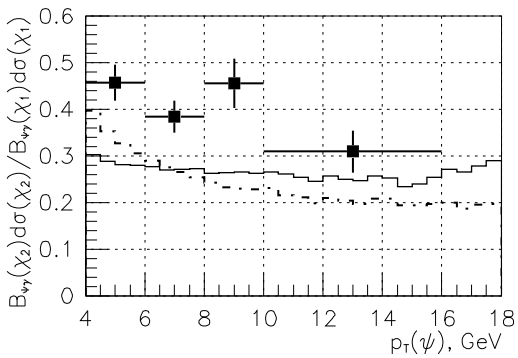

FIG. 4: Leading-order colinear predictions on the visible ratio of χ_{cJ} contributions to J/ψ production at the Tevatron: solid line, under the hypothesis of electric dipole transitions; dash-dotted line, for uniform (unpolarized) decay distributions. ■ CDF data [1].

differential cross sections is guaranteed by the shape of the gluon densities. The latter is determined by the t-channel gluon propagators in the gluon evolution and scales as $1/p_T^4$. We have already seen good agreement with the data in Fig. 5.

Fig. 6 displays our predictions on the χ_{c1} and χ_{c2} cross sections and their ratio. The suppression of χ_{c1} states at low p_T is motivated by Landau-Yang theorem, while at larger p_T the suppression goes away. Here we

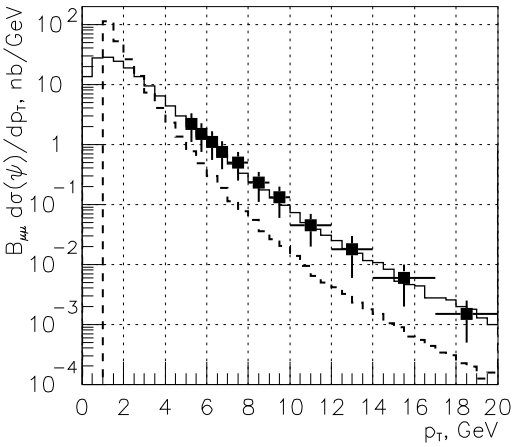

FIG. 5: Transverse momentum distribution of J/ψ mesons produced in radiative decays $\chi_{cJ} \to J/\psi+\gamma$ at the Tevatron, $\sqrt{s} = 1.8$ TeV, $|\eta(J/\psi)| < 0.6$. Solid histogram, k_t-factorization approach with JB [7] gluon densities; dashed histogram, collinear parton model with GRV [6] gluon densities; ■ CDF data [13].

see the effect of initial gluon off-shellness which is essentially the effect of the gluon longitudinal polarization not subject to Landau-Yang selection rule. The ratio $d\sigma(\chi_{c1})/d\sigma(\chi_{c2})$ then tends to a constant value, but the asymptotic value is different from the one obtained in collinear calculations. Most probably, this difference has to be attributed to the diagrams of the type Fig. 1(b) and (d). These diagrams are only present in the collinear but not the k_t-factorization approach, while the diagram of the type Fig. 1(c) is effectively included as part of the gluon evolution (Fig. 1(a)).

The polarization pattern (Fig. 7) is qualitatively similar to that observed in the collinear case, and the resulting ratio of the χ_{cJ} contributions is presented in Fig. 8. Polarization produces a noticeable, though not dramatic effect; but whether it is taken into account or not, our predictions lie well outside the experimental errors.

We can extract one positive lesson that employing the 2→2 subprocess (2) leads to better proportion between the χ_{cJ} yields. So, let us try incorporating this subprocess with the k_t-factorization scheme. Now we calculate the appropriate matrix elements with off-shell initial gluons and convolute it with unintegrated gluon distributions. Similarly to the already discussed LO case, the p_T behavior of this contribution is determined by the shape of the gluon densities and scales as $1/p_T^4$.

The results based on the subprocess (2) taken solely look still not satisfacory (Fig. 9). And, besides that, is not clear enough how to correctly add the contributions from subprocesses (1) and (2) avoiding the danger of double counting between the formally LO diagram of Fig. 1(a) and formally NLO diagram of Fig. 1(c). The problem of including the NLO contributions is yet an unresolved problem in the k_t-factorization.

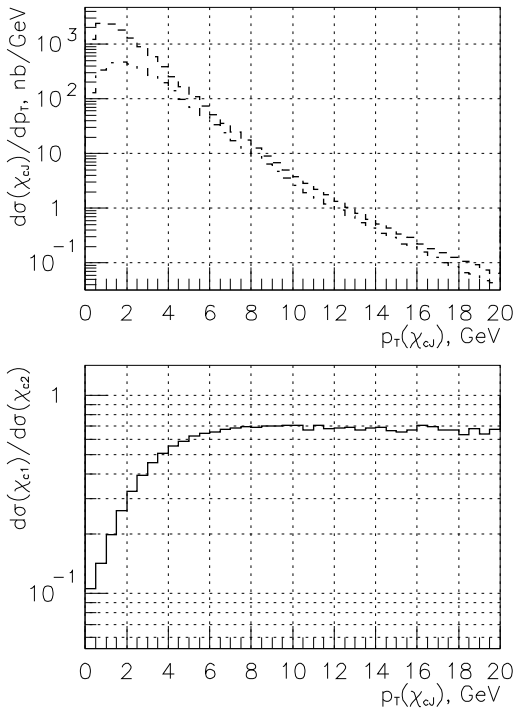

FIG. 6: Predictions of the k_t-factorization approach for the Tevatron conditions: $\sqrt{s} = 1.96$ GeV, $|\eta(\chi_{cJ})| < 1$. Upper panel, transverse momentum distributions of the χ_{c1} (dash-dotted line) and χ_{c2} (dashed line) mesons. Lower panel, the ratio of the χ_{c1} and χ_{c2} production cross sections.

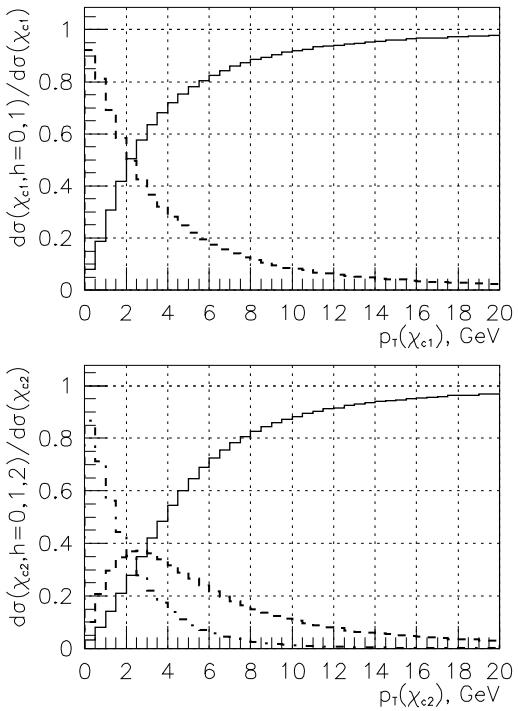

FIG. 7: k_t-factorization predictions on the χ_{cJ} spin alignement parameters at the Tevatron as seen in the helicity frame. Upper panel, χ_{c1} mesons; lower panel, χ_{c2} mesons. Solid lines, $h = 0$ states; dashed lines, $|h| = 1$ states; dash-dotted line, $|h| = 2$ states.

But there exists yet another way to solve the puzzle, and it looks rather natural and attractive. Up to now, we were considering the χ_{c1} and χ_{c2} wave functions as identical, $|\mathcal{R}'_{\chi 1}(0)|^2 = |\mathcal{R}'_{\chi 2}(0)|^2$. This might be an oversimplification, because the underlying potential models [15]-[18] ignore the spin-orbital interaction and consider quarks as essentially scalar objects. We know, on the other hand, that the mass of χ_{c1} state is lower than that of χ_{c2}, and it means that the quark-antiquark binding in the χ_{c1} system is tighter. No wonder if the corresponding wave function is narrower and higher.

It is worth mentioning another interesting property. Contrary to the spin counting expectations, the decays $\psi(2S) \to \chi_{cJ}+\gamma$ do not populate the χ_{c1} and χ_{c2} states in proportion to the number of spin degrees of freedom, i.e., 3:5, but rather in proportion 1:1 [19]. This property holds for both charmonium and bottomonium families: $Br(\psi_{(2S)}\to\chi_{c1}\gamma) \simeq Br(\psi_{(2S)}\to\chi_{c2}\gamma)$, as well as $Br(\Upsilon_{(2S)}\to\chi_{b1}\gamma) \simeq Br(\Upsilon_{(2S)}\to\chi_{b2}\gamma)$ and $Br(\Upsilon_{(3S)}\to\chi_{b1(2P)}\gamma) \simeq Br(\Upsilon_{(3S)}\to\chi_{b2(2P)}\gamma)$.

The estimate 3:5 may seem too naive, but it can be obtained in a more accurate way. Assume that the $\psi(2S) \to \chi_{cJ}+\gamma$ transition amplitudes factorize into coordinate-dependent and spin-dependent parts. The coordinate-dependent factors are determined by the $\psi(2S)$ and χ_{cJ} wave functions, and if the χ_{c1} and χ_{c2} wave functions are

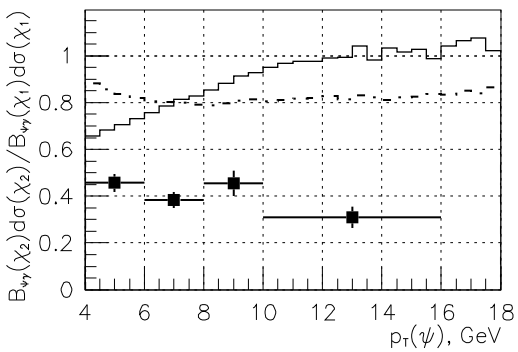

FIG. 8: k_t-factorization predictions on the visible ratio of χ_{cJ} contributions to J/ψ production at the Tevatron: solid line, under the hypothesis of electric dipole transitions; dash-dotted line, for uniform (unpolarized) decay distributions; ■ CDF data. [1].

identical the respective amplitudes should also be equal. Now, to compare the spin-dependent factors, we calculate the projections of the $\psi(2S)$ state onto $\chi_{cJ}+\gamma$ states using the Clebsch-Gordan coefficients. Here we keep in mind that the photon has two (not three) helicity states and, consequently, not all of the $|J, m\rangle$ states are equally allowed for χ_{c1} and χ_{c2} mesons. Summing up, we get $\Gamma(\psi_{(2S)}\to\chi_{c1}\gamma)$: $\Gamma(\psi_{(2S)}\to\chi_{c2}\gamma) = 2{:}(10/3) = 3{:}5$.

There should be some reason for the fact that in reality

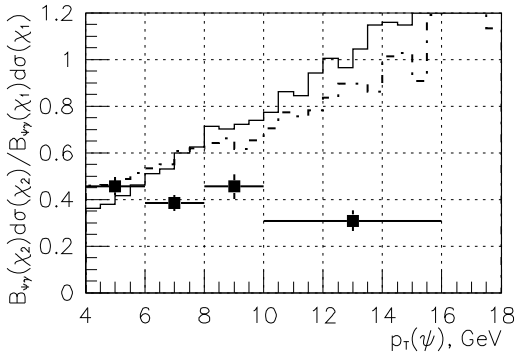

FIG. 9: Predictions on the visible ratio of χ_{cJ} contributions to J/ψ based on the sole subproces $g + g \to \chi_{cJ} + g$ considered in the k_t-factorization scheme. Solid line, under the hypothesis of electric dipole transitions; dash-dotted line, for unpolarized decay distributions; ■ CDF data [1].

the proportion between the χ_{c1} and χ_{c2} yields is shifted in favor of χ_{c1}, and we suggest it could be the difference between the χ_{cJ} wave functions. Having the wave functions rescaled as $|\mathcal{R}'_{\chi 1}(0)|^2 : |\mathcal{R}'_{\chi 2}(0)|^2 = 5 : 3$ and introducing the correction factor in the plots of Fig. 8 we arrive at a quite satisfactory agrement with the data.

IV. COMPARISON TO THE HERA-B DATA

At the conditions of fixed-target experiments, all calculations are on poorer theoretical grounds. Firstly, we need to say that the conventional collinear approach is unsuitable in this case because of singularities in the matrix elements. The χ_{c2} production cross section diverges when p_T goes to zero, but, in contrast with the Tevatron situation, this region lies within the experimental aceptance.

Secondly, the typical values of the Bjorken variable x are not small: $< x > \simeq m_\chi/\sqrt{s} \simeq 0.1$. By far, they lie beyond the "small-x" domain the k_t-factorization approach is aimed at. Extrapolations of unintegrated gluon distributions fitted to high-energy (e.g., small-x) data may differ significantly in the large-x region making theoretical predictions rather uncertain.

An illustration can be seen in Fig. 10. While the predictions based on the JB and A0 gluon parametrizations were very close to each other at the Tevatron conditions, they differ by about a factor of 30 for HERA-B.

The restrictions on the photon energy and transverse momentum are so soft ($E(\gamma) > 0.3$ GeV, $E_T(\gamma) > 0.2$ GeV) that only as few as 15% of the events are rejected by these cuts. The effects of polarization, though interesting on their own, have no effect on the detection efficiency.

Using the A0 gluon distribution we estimate the integral production cross sections as $\sigma(\chi_{c1}) = 160$ nb and $\sigma(\chi_{c2}) = 850$ nb. Using the JB gluon distribution we get $\sigma(\chi_{c1}) = 4.2$ nb and $\sigma(\chi_{c2}) = 29$ nb. This has to be compared with the experimental result [2] $\sigma(\chi_{c1}) = 133 \pm 35$ nb/nucleon and $\sigma(\chi_{c1}) = 231 \pm 61$ nb/nucleon.

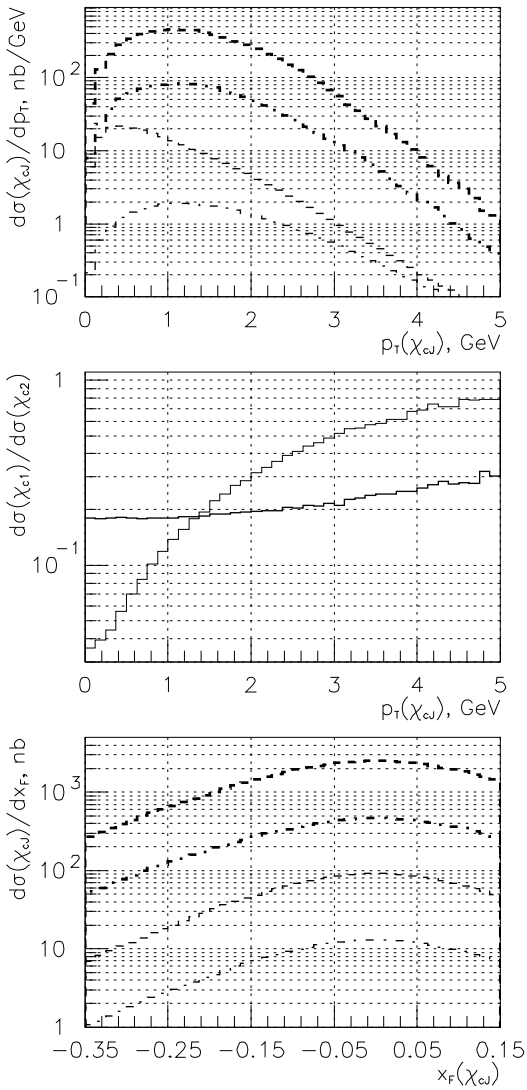

FIG. 10: Predictions of the k_t-factorization approach for the DESY HERA-B conditions: $\sqrt{s} = 41.6$ GeV, $-0.35 < x_F(\chi_{cJ}) < 0.15$. Upper panel, transverse momentum distributions of the χ_{c1} (dash-dotted) and χ_{c2} (dotted) mesons; middle panel, the ratio of the differential cross sections; lower panel, χ_{c1} (dash-dotted) and χ_{c2} (dotted) production cross sections as functions of x_F. Thin lines, JB [7] gluon distributions; thick lines, A0 [8] gluon distributions.

Here in the unrestricted phase space, Landau-Yang suppression comes in force in full measure, and we obtain $\sigma(\chi_{c1})/\sigma(\chi_{c2}) = 0.19$ for A0 gluons and $\sigma(\chi_{c1})/\sigma(\chi_{c2}) = 0.15$ for JB gluons, with both predictions looking incompatible with the experimental measurement [2] $\sigma(\chi_{c1})/\sigma(\chi_{c2}) = 0.57$.

The only excuse we can suggest is that the experimental systematical errors are probably much larger than estimated by the authors of [2]. Since a photon from a χ_{cJ} decay cannot be distinguished from the others in the

event, the experiment has as low signal-to-background ratio as 1:20 (see Figs. 5 and 6 in Ref. [2], where the signal is hardly recognizable by unaided eye). Also, the energy resolution of the detector is worse than the distance between the χ_{c1} and χ_{c2} masses. The mesons are not seen as separate peaks in the $l^+l^-\gamma$ invariant mass spectrum, but merge together into a single bump. The individual contributions from χ_{c1} and χ_{c2} states were only obtained by using a fit with two Gaussians centered at predefined mass values.

V. CONCLUSIONS

We have considered the production of χ_{cJ} mesons at the conditions of the CDF and HERA-B experiments and analyzed the role of several factors that can affect the predicted ratio of the production rates. We have studied the effect of χ_{cJ} polarization, the effect of next-to-leading order contributions, and the effect of probably different χ_{c1} and χ_{c2} wave functions. In all cases the experimental restrictions have been properly included in the analysis. Polarization was found to be important, though not critical for understanding the data.

As far as the collinear scheme is concerned, the leading order calculations showed inadequate p_T dependence of the production cross sections. We have also learned from the literature that performing the full next-to-leading order (NLO) calculations revealed inconsistency of the purely perturbative approach, as the calculated cross sections were negative. The positivity of the cross sections could only be reached by involving the nonperturbative color-octet contributions. Thus, the whole problem turned out to be essentially nonperturbative and hardly manageable in the framework of the theory.

On the contrary, with the k_t-factorization approach we can keep staying in the perturbative domain. However, including the next-to-leading order contributions turned out to be not helpful in reaching agreement with the data. And, in addition to that, it met internal theoretical difficulties.

The most likely explanation of the Tevatron data suggests that the wave functions of χ_{c1} and χ_{c2} states are different. Another evidence for this property comes from the fact that the decays $\psi(2S) \to \chi_{cJ}+\gamma$ do not populate the χ_{c1} and χ_{c2} states in proportion to the number of spin degrees of freedom 3:5, but in proportion 1:1.

Our predictions on the ratio of the χ_{cJ} yields at the HERA-B conditions disagree with the experimental result by a factor of 3. It is yet unclear to us whether this discrepancy indicates some defect in the theoretical scheme or can be attributed to huge combinatorial background and bad energy resolution in the experiment.

ACKNOWLEDGMENTS

The author conveys his thanks to Hannes Jung and Nikolai Zotov for their encouraging interest and useful discussions.

This work was supported by the Presidium of Russian Academy of Sciences in the framework of the program "Experimental and theoretical investigations of fundamental interactions at the LHC" and by DESY Directorate in the framework of Moscow-DESY project on Monte-Carlo implementation for HERA-LHC.

[1] A. Abulencia *et al.* (CDF Collaboration), Phys. Rev. Lett. **98**, 232001 (2007).
[2] I. Abt *et al.* (HERA-B Collaboration), Phys. Rev. D **79**, 012001 (2009).
[3] H. Krasemann, Z. Phys. C **1**, 189 (1979); G. Guberina, J. Kühn, R. Peccei, and R. Rückl, Nucl. Phys. **B174**, 317 (1980).
[4] S. P. Baranov, Phys. Rev. D **66**, 114003 (2002).
[5] B. Kniehl, G. Kramer, and C. Palisoc, Phys. Rev. D **68**, 114002 (2003).
[6] M. Glück, E. Reya, and A. Vogt, Eur. Phys. J. C **5**, 461 (1998).
[7] J. Blümlein, DESY Report No.95-121, 1995; J. Phys. G **19**, 1623 (1993).
[8] H. Jung, http://www.desy.de/∼jung/cascade/updf.html
[9] M. Ciafaloni, Nucl. Phys. **B296**, 49 (1998); S. Catani, F. Fiorani, and G. Marchesini, Phys. Lett. B **234**, 339 (1990); Nucl. Phys. **B336**, 18 (1990); G. Marchesini, Nucl. Phys. **B445**, 49 (1995).
[10] E. J. Eichten and C. Quigg, Phys. Rev. D **52**, 1726 (1995).
[11] S. P. Baranov, N. P. Zotov, JETP Lett. **86**, 435 (2007).
[12] P. Cho, M. Wise, and S. Trivedi, Phys. Rev. D **51**, R2039 (1995).
[13] F. Abe *et al.* (CDF Collaboration), Phys. Rev. Lett. **79**, 578 (1997).
[14] Y.-Q. Ma, K. Wang, and K.-T. Chao, arxiv:1002.3987.
[15] W. Buchmüller and S.-H. Tye, Phys. Rev. D **24**, 132 (1981).
[16] A. Martin, Phys. Lett. B **93**, 338 (1980).
[17] C. Quigg and J. L. Rosner, Phys. Lett. B **71**, 153 (1977).
[18] E. Eichten, K. Gottfried, T. Kinoshita, K. D. Lane, and T.-M. Yan, Phys. Rev. D **17**, 3090 (1978); **21**, 313(E) (1980); **21**, 203 (1980).
[19] K. Nakamura *et al.* (Particle Data Group), J. Phys. G **37**, 075021 (2010).